Polymer Brushes: Probing the Collapse Dynamics of Poly(N-isopropylacrylamide) Brushes by AFM: Effects of Co-nonsolvency and Grafting Densities (Small 10/2011)

ARTICLE *in* SMALL · MAY 2011

Impact Factor: 8.37 · DOI: 10.1002/smll.201002229 · Source: PubMed

4 AUTHORS, INCLUDING:

Xiaofeng Sui
University of Twente
30 PUBLICATIONS **605** CITATIONS
SEE PROFILE

Qi Chen
Royal DSM
10 PUBLICATIONS **156** CITATIONS
SEE PROFILE

Gyula Julius Vancso
University of Twente
277 PUBLICATIONS **6,430** CITATIONS
SEE PROFILE

Probing the Collapse Dynamics of Poly(*N*-isopropylacrylamide) Brushes by AFM: Effects of Co-nonsolvency and Grafting Densities

*Xiaofeng Sui, Qi Chen, Mark A. Hempenius, and G. Julius Vancso**

Collapse of poly(N-isopropylacrylamide) (PNIPAM) brushes in the mixed solvent system (water/methanol 50% v/v) is studied by in-situ atomic-force microscopy (AFM). PNIPAM brushes with three different grafting densities and similar chain lengths are synthesized via surface-initiated atom-transfer radical polymerization. By changing the solvent from water to a water/methanol (50% v/v) mixture, the polymer brushes switch from a swollen to collapsed state. AFM force measurements using a silica colloidal probe attached to the tip are employed to obtain the Young's moduli of the polymer brushes in different solvation states. The collapse dynamics of the brush is followed by monitoring the pull-off force (adherence) in situ. The modulus of the swollen high-density polymer brush is four times lower than that of the same brush in the collapsed state. It is shown that in the case of the high-density polymer brush with a thickness ($t_{\text{in water}}$) of 900 nm, the collapse takes place in a time scale of ~25 s, whereas the collapse occurs faster for the medium-density brush ($t_{\text{in water}}$ = 630 nm) and much more rapidly for the low-density brush ($t_{\text{in water}}$ = 80 nm). This difference in the response kinetics is primarily ascribed to the time needed for solvent exchange in the polymer brushes.

1. Introduction

Stimuli-responsive polymer brushes made of surface-tethered macromolecules have been widely applied to prepare sensors, to regulate cell culture, to control wetting and adhesion, and in many other areas.[1–8] Small changes in the external environment (e.g., temperature, pH, or ionic strength) can generally trigger a sharp and large response in the structure and properties of these grafted polymer brushes. Various polymer brushes have been synthesized via the surface-initiated atom-transfer radical polymerization (SI-ATRP) approach from different substrates using surface-attached initiators. This method allows one to accurately control the structure and properties of the polymer grafts.[2] Poly(*N*-isopropylacrylamide) (PNIPAM) has been widely studied as a thermally responsive polymer since its lower critical solution temperature (LCST, ≈32 °C) is around physiological temperature.[9,10] PNIPAM chains show strong hydration behavior below the LCST, while above the LCST they adopt a dehydrated and compact form. By utilizing the hydration/dehydration effect, PNIPAM brushes are expected to have applications in, for example, permeation-controlled filters, tissue engineering, and actuators.[11] The influence of temperature on the polymer structure and hydration of PNIPAM brushes is well documented in the literature.[12–25] Several methods, including atomic force microscopy (AFM), surface force measurements, neutron reflectivity, quartz-crystal microbalance, and surface plasmon resonance, have been used to monitor the reversible change of surface thermoresponsive properties for PNIPAM films with different densities and molar masses.[12–25]

X. Sui,[+] Dr. Q. Chen,[+] Dr. M. A. Hempenius, Prof. G. J. Vancso
Department of Materials Science and Technology of Polymers
University of Twente
MESA+ Institute for Nanotechnology
P.O. Box 217, 7500 AE Enschede, The Netherlands
E-mail: g.j.vancso@tnw.utwente.nl
[+] These authors contributed equally to this work.

DOI: 10.1002/smll.201002229

small NANO MICRO

PNIPAM is also known to exhibit co-nonsolvency behavior, that is, solvation responsiveness to the variation in the composition of mixed solvents consisting of water and certain water-miscible organic solvents such as alcohols.[26–28] At a temperature below its LCST, PNIPAM can be dissolved in pure water as well as in these organic solvents, but it will precipitate in some solvent mixtures at certain volume ratios. This so-called co-nonsolvency effect is of substantial technological relevance in applications such as actuators and microfluidics. However, the co-nonsolvency effect for well-defined PNIPAM polymer brushes has received very limited attention.[29–31]

AFM and nanoindentation[32] allow one to measure the local hardness and the elastic properties of polymer films with thicknesses in the range from a few tens to hundreds of nanometers. AFM has also been used with success to image the surface morphology of polymer brushes, measure their height, and determine their surface adhesion as well as brush modulus.[33] For instance, the pull-off force of an AFM silicon nitride tip from a PNIPAM brush surface was recorded when the brushes were swollen (below the LCST) or collapsed (above the LCST) and a difference in the adhesion was observed.[14] In another example, topography and microtribological properties of Y-shaped binary polymer brushes made of polystyrene and poly(acrylic acid) were studied by AFM. It was found that these polymer brushes exhibited a dramatic variation in topography as well as adhesive, elastic, and frictional properties under different solvents.[34,35] Another important aspect in AFM-related studies is the study of time-dependent processes. Research showed that the dynamic response of grafted polymer brushes to environmental changes could be followed using AFM. In a recent case, Ryan et al. directly visualized the swelling and collapse of a poly(methacrylic acid) brush by monitoring the change in the height of a patterned brush layer under different pH values.[36]

In the above-mentioned examples, the dynamic responses of polymer brushes were studied primarily by monitoring the change in thickness of the polymer brush. Herein, we measured the adherence of PNIPAM brushes to an AFM colloidal probe. Adherence is an important parameter for the utilization of stimulus-responsive brushes in various applications, such as wetting and adhesion control.[37] Adherence was monitored by recording AFM force curves during the collapse of the brush induced by the addition of co-nonsolvent. To our knowledge, this is the first time that the dynamics of adherence variation associated with molecular rearrangements during a phase transition of a responsive polymer brush was directly monitored using AFM. PNIPAM brushes with three different grafting densities were synthesized via SI-ATRP. The polymerizations were initiated by reactive alkylsilane initiators which were covalently coupled to the silicon substrates in the form of thin molecular layers (see **Scheme 1**).[38,39] The values of Young's moduli of PNIPAM brushes under different solvent conditions were estimated based on the Hertz model using AFM force–distance curves.

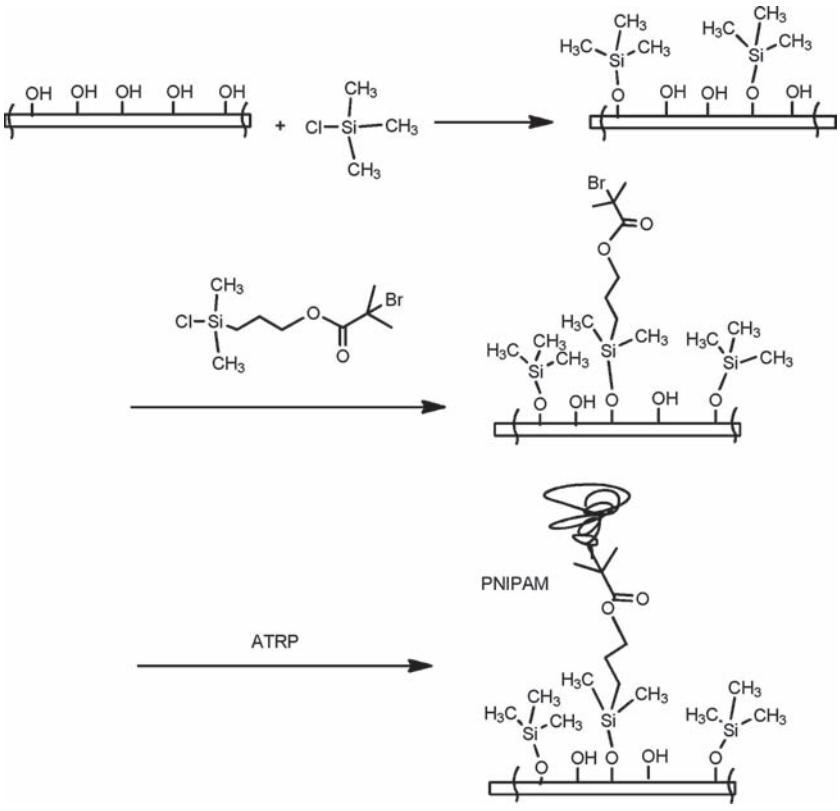

Scheme 1. Schematic representation of grafting PNIPAM on silicon substrates.

2. Results and Discussion

2.1. Synthesis of PNIPAM Brushes with Different Grafting Densities

Three brush samples exhibiting different grafting densities were studied (for brush characteristics see **Table 1**). "Grafting from" of brushes was achieved using chlorosilane-terminated initiators, which were deposited into the defect sites of previously prepared inert alkylchlorosilane monolayers on silicon. This sequential method[40] allowed us to achieve homogeneous coverage of the initiating species with different grafting densities. We note that prior to polymerization, the surfaces

Table 1. Thickness in dry, swollen, and collapsed states and estimated grafting density of the PNIPAM polymer brushes.

	t_{dry} [nm]	$t_{in\ water}$ [nm]	$t_{in\ water/methanol\ (50\%\ v/v)}$ [nm]	d (est.) [chains nm^{-2}]
LD PNIPAM	10	80	20	0.03
MD PNIPAM	100	630	200	0.27
HD PNIPAM	240	900	440	0.69

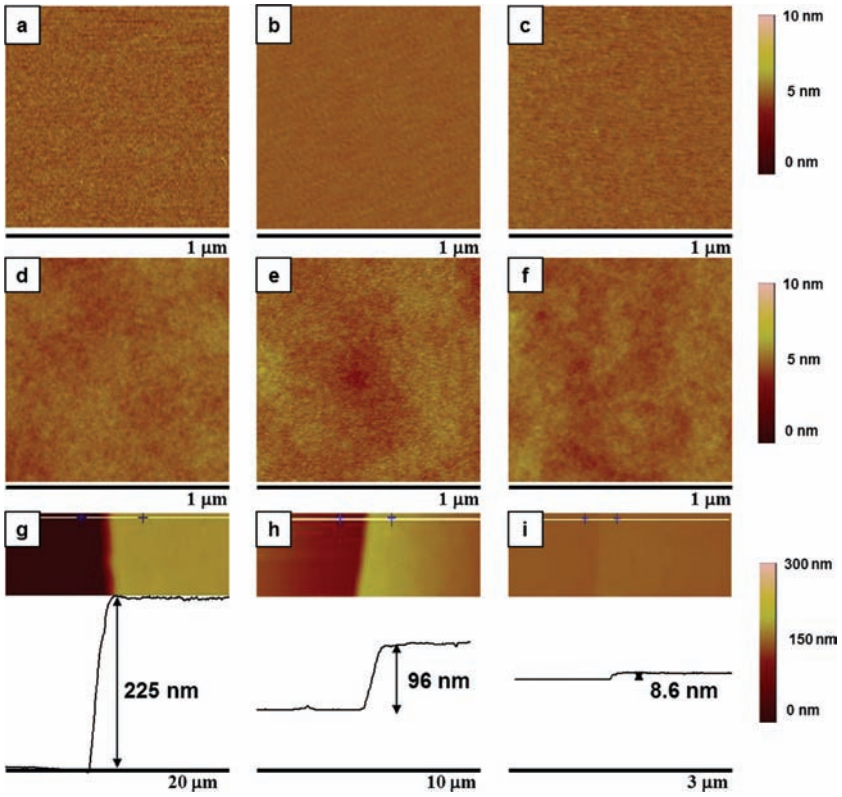

Figure 1. Tapping mode AFM height images in air of the a) 3-(chlorodimethylsilyl)propyl 2-bromo-2-methylpropionate (CDB) deposited (HD) surface, b) chlorotrimethylsilane (CTS)/CDB deposited (MD) surface, c) CTS/CDB deposited (LD) surface, and subsequently PNIPAM brush on the d) HD, e) MD, and f) LD surfaces, as well as height images and cross sections of scratches to measure the PNIPAM film thickness grafted from the g) HD, h) MD, and i) LD surfaces.

of the substrates featuring the initiators did not exhibit any evident segregation, which suggests a homogeneous monolayer (**Figure 1**a–c).

We studied three different brushes with various densities, which are termed high-, middle-, and low-density (HD, MD, and LD, respectively) surfaces. The polymerization time was 30 min for each sample. Variation of the initiator coverage, which determines the graft density, was achieved by varying the immersion time of the substrates in the solution of inert silanes (see Experimental Section). The surface morphology and brush height were imaged by tapping mode AFM for the three brushes investigated (Figure 1d–i). The grafts showed a smooth surface with a low roughness value ranging within 0.3 nm for scan sizes of $1 \times 1\ \mu m^2$. AFM cross-sectional profiles yielded brush height values (for dry thicknesses) of 225 (HD), 96 (MD), and 9 nm (LD), respectively (Figure 1g–i). The formation of PNIPAM grafts was also confirmed by FTIR spectroscopy (see Supporting Information), ellipsometry, and contact angle measurements. Surface analysis by ellipsometry demonstrated the formation of PNIPAM brushes with a height of 240 ± 1 nm for HD, 100 ± 1 nm for MD, and 10 ± 1 nm for LD surfaces. These values are in good agreement with the AFM data (Table 1). Static contact angle (SCA) measurements using MilliQ water showed values of $56 \pm 2°$ for all samples regardless of the brush height, which is typical for PNIPAM films.[41] This indicates that the wetting is mainly sensitive to the chemical composition of the outermost region of the layers.[21] As identical conditions were applied for all polymerizations, we assumed that different samples have similar molar masses and polydispersity values for the grafted chains. The grafting density (Table 1) of the PNIPAM brush was estimated[13,42] by measuring the dry thickness and molar mass of the free polymer (M_n= 219 600 g mol^{-1}; M_w = 519 300 g mol^{-1}) obtained using "sacrificial initiators" in the polymerization mixture.[43] In-situ ellipsometry studies[44–45] were performed to examine the swelling of these PNIPAM brushes in water. When swelled in deionized water at 22 °C, the height of the HD sample increased from 240 to 900 nm, for MD PNIPAM from 100 to 630 nm, while in the case of the LD sample it increased from 10 to 80 nm.

2.2. AFM Force Measurements on PNIPAM Brushes

To study the impact of co-nonsolvency as well as variation of the brush height on the mechanical properties of the PNIPAM brushes, force versus distance profiles were acquired by AFM to probe the structure and tip–brush interactions by using the colloidal probe approach.[46] This technique was proved useful for the quantification of surface forces for various soft-matter systems.[37,47,48] The colloidal particle attached to the tip was a silica sphere with a radius of 500 nm (see Experimental Section). Typical raw data showing the approach section of deflection versus piezo-extension curves for the PNIPAM brushes are shown in **Figure 2**. The data were constructed based on ten individual force curve measurements.

As shown in Figure 2, the deflection of the AFM cantilever changed when the PNIPAM brushes were exposed to different solvent conditions. The interaction between the colloidal probe and the surface was repulsive when the polymer was swollen, while it became attractive and jump-to-contact behavior was observed when the solvent environment was changed to a water/methanol (50% v/v) mixture, regardless of differences in brush height. Such changes in tip–surface interactions as PNIPAM is brought across the LCST by changing the temperature have been documented in the literature[14] and are also observed here by inducing the transition using a co-nonsolvent. A difference in the slope of the curves after contact is clearly observed when either the grafting density of the PNIPAM brushes is changed or when the solvent composition is varied. To elucidate this difference in a quantitative way, the apparent Young's modulus of the PNIPAM brush was determined from the recorded curves based on the Hertz model.[37]

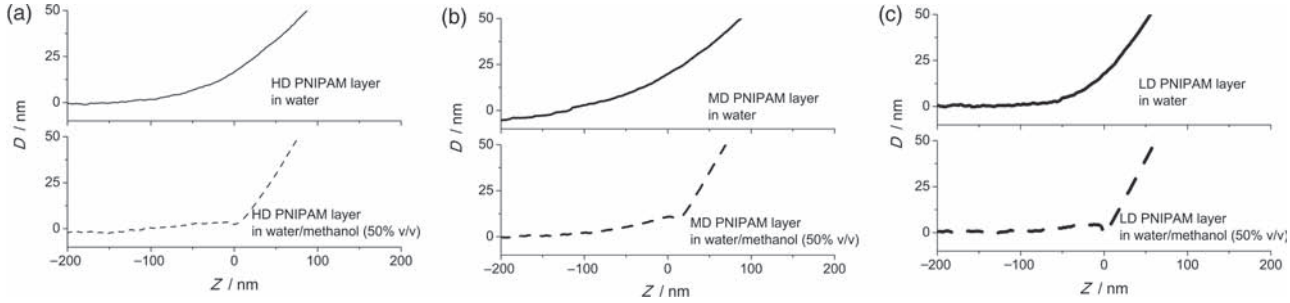

Figure 2. AFM cantilever approach deflection versus extension curves for PNIPAM brushes with different grafting densities under different solvent conditions as indicated.

From the approach part of the deflection–extension curves the deformation of the PNIPAM grafts can be obtained. Deformation (δ) is calculated from Equation (1):

$$\delta = |Z - Z_0| - (D - D_0) \quad (1)$$

where Z denotes the piezo-extension, Z_0 is the piezo-extension at which tip–surface contact occurs, and D and D_0 are the values of deflection of the cantilever and deflection of the cantilever when tip–surface contact occurs, respectively. The load (F) applied onto the polymer brush is then calculated from Equation (2):

$$F = k(D - D_0) \quad (2)$$

where k represents the spring constant of the AFM cantilever, which is calibrated using the thermal tune function of the instrument software. The Hertz equation [Eq. (3)] was used to determine the values of the apparent Young's modulus:

$$F = \frac{4\sqrt{r_{tip}}}{3(1-\nu^2)} E \cdot \delta^{3/2} \quad (3)$$

where r_{tip} is the radius of the silica colloidal probe, ν is the Poisson ratio, and E is the apparent Young's modulus of the polymer brush (assuming an infinitely higher modulus of the probe as compared to the brush). Typical Hertz plots, in which F was displayed as a function of $\delta^{3/2}$, are shown in **Figure 3**a–c for PNIPAM brushes with different brush heights under different solvent conditions. (The charts were constructed based on ten individual measurements.[49])

As can be seen in Figure 3, PNIPAM brushes are more deformable in water (filled symbols), that is, deformation is higher at a certain load, than in a water/methanol (50% v/v) mixture (open symbols), regardless of the brush heights. This is explained by the fact that under mixed solvent conditions, the polymer chains collapse onto the surface while in water the polymer chains are expanded. A notable difference in the deformation under the same load was also observed for PNIPAM brushes with different brush heights under the same solvent conditions. For the LD and MD brushes, the grafts were flattened laterally more than the HD sample. This was evidenced by thickness measurements using in situ ellipsometry. The situation is schematically shown in Figure 3d.

To accurately predict the elastic behavior of the PNIPAM brushes, the initial 20% of the δ value was used to evaluate the apparent Young's modulus. We assumed a Poisson ratio of 0.5 and the radius of the colloidal probe (500 nm) was determined by scanning the probe with a tip calibration array. The value of the apparent Young's modulus of the PNIPAM brushes[50,51] was then calculated. Histograms (N = 50) of the distributions of the Young's modulus values with different grafting densities under different solvent conditions are shown in **Figure 4**.

The arithmetic mean value of the apparent Young's modulus of the HD sample in water is 123 ± 9 kPa, while the values of the apparent Young's modulus of the MD and LD samples in water are 150 ± 4 and 394 ± 55 kPa, respectively. In a water/methanol (50% v/v) mixture the modulus value is substantially higher: for the HD sample 500 ± 69 kPa, for the MD sample 688 ± 108 kPa, and for the LD sample 1662 ± 358 kPa were found. This fourfold increase of the apparent Young's modulus as the PNIPAM brush is changed from the swollen to the collapsed state corresponds well to literature findings.[52–54] Furthermore, a higher value of the apparent Young's modulus was observed for the LD PNIPAM grafts as compared to the HD and MD samples. This could be ascribed to the influence of the silicon substrate underneath the polymer brushes,[55–57] even though only the top 20% of the deformation was used to evaluate the data.[58] In addition, as for the LD sample the grafting density was relatively low, structural heterogeneities over the contact area may exist, which could increase the apparent modulus value due to the influence of the stiffer substrate. The presence of contact area heterogeneities could also explain why a broader distribution was obtained for the LD sample.

2.3. Monitoring the Collapse Dynamics of PNIPAM Brushes

In order to study the dynamics of the switching of PNIPAM brushes from the swollen to the collapsed state, the adherence (pull-off force)[59] between the sample surface and the AFM colloidal probe was monitored by recording force curves at constant time intervals. The change in the polymer chain conformation and swelling

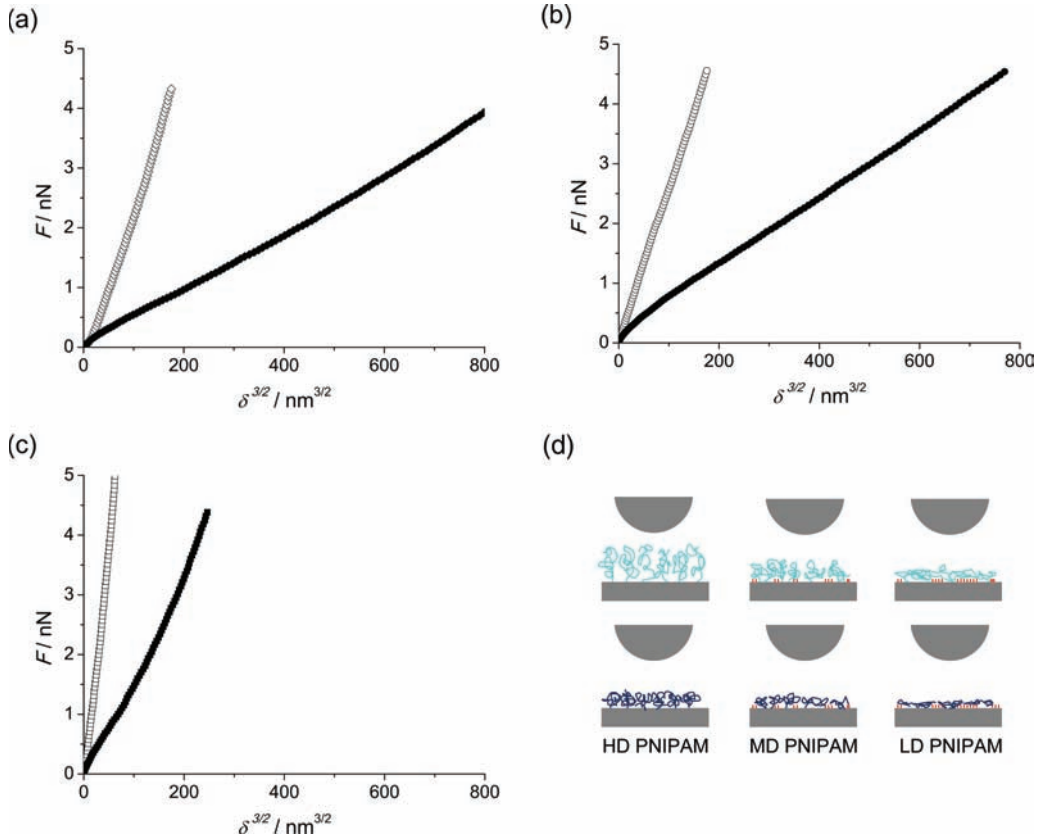

Figure 3. Hertz plots of PNIPAM a) HD, b) MD, and c) LD brushes under water (filled symbols) and water/methanol (50% v/v, open symbols). d) Schematic representation of the contact between the colloidal AFM probe and the PNIPAM brush with different grafting densities under different solvent conditions.

state causes a change in adherence between the polymer and the AFM probe, as reported earlier.[14] Here the value of the pull-off force was determined from the retract part of the force curve, which is shown in the insets of **Figure 5**a. The obtained pull-off forces between the HD, MD, and LD PNIPAM brushes and the probe were then plotted as a function of time and are displayed in Figure 5a–c.

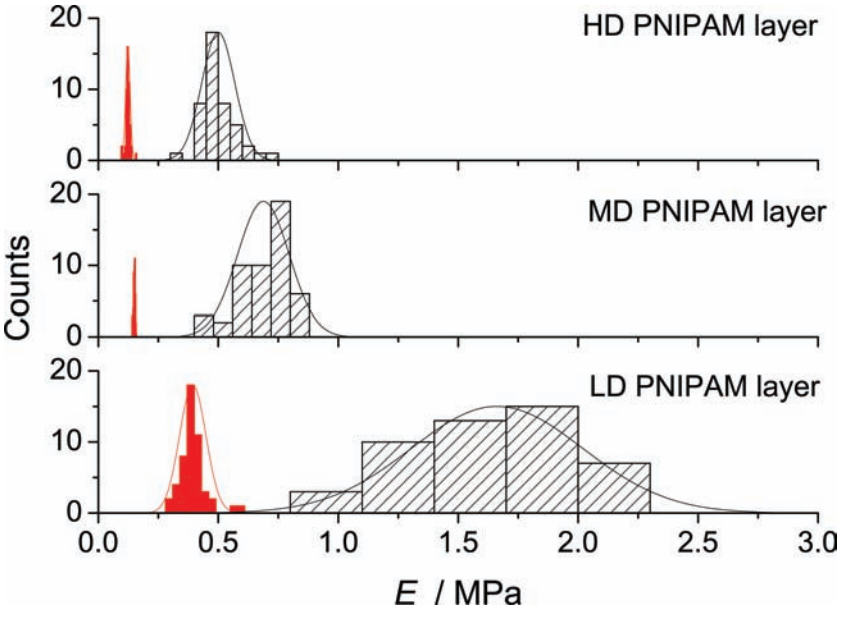

Figure 4. Statistical histograms of the Young's modulus of PNIPAM brushes in water (filled) and in water/methanol (50% v/v; patterned).

Initially the adherence between the brushes and the probe was essentially zero for all grafting densities due to steric interaction between the brush and the probe.[60] After introducing the co-nonsolvent (i.e., water/methanol, 50% v/v) as indicated by the gray bars in Figure 5, the interaction became attractive and pull-off forces on the order of a few tens of nano-Newtons were recorded. The value of the pull-off force generally increased as the thickness of the PNIPAM brush increased. This again confirms the transition of PNIPAM chains from swollen to collapsed states due to the co-nonsolvency effect. (We note that another brush system consisting of poly(2-(methacryloyloxy) ethyl phosphorylcholine) (PMPC) brushes as one of the first examples exhibiting a co-nonsolvency effect in any polymer brush, observed by ellipsometry, has been only recently reported.[44])

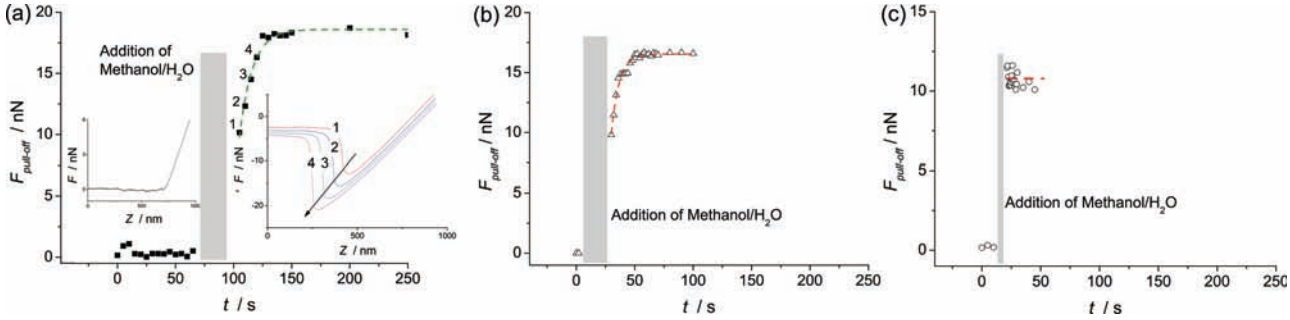

Figure 5. Evolution of pull-off forces between the colloidal AFM tip and the a) HD, b) MD, and c) LD PNIPAM surfaces. The gray bar indicates the change of solvent environment from pure water to water/methanol (50% v/v) mixture. The retract force–extension curves on the HD PNIPAM brush before and after the solvent change are also shown as insets in (a).

Changing the solvent environment back to pure water caused the attractive adherence forces to disappear, which indicated the reversibility of the process. However, no clear kinetics could be observed in the case of swelling, as equilibration of the system took a very long time and no stable AFM force curves could be recorded. Thus instead of measuring swelling, the collapse dynamics of the PNIPAM brushes was monitored.

As shown in Figure 5a, the pull-off force for the HD sample gradually increased over a period of 25 s from 0 to a plateau value of 19 nN. The collapse dynamics for the LD sample could not be resolved (Figure 5c) as after the addition of co-nonsolvent the pull-off force immediately reached the equilibrated value of 11 nN. An intermediate kinetics of the transition was observed for the MD sample, as the adhesion reached the equilibrated 16 nN value in roughly 18 s. It should be noted that the precise time of the collapse can be longer as the transition was already initiated while the co-nonsolvent was introduced (gray bar). A typical equilibration time for the HD and MD samples was 40 s, while the LD sample equilibrated within 5 s. Regardless, a clear and direct correlation could be observed between the collapse dynamics and the brush thicknesses of the PNIPAM grafts. We attribute this finding to the diffusion of solvent molecules into (or out of) the PNIPAM brushes. In the case of a thicker polymer brush, more time is needed for solvent exchange to take place as the collapsed outer layer serves as a diffusion barrier. It should be noted that in a recent study, the collapse transition of poly(di(ethylene glycol) methyl ether methacrylate) ($PMEO_2MA$) was monitored using quartz crystal microbalance and contact angle measurements.[61] It was found that the transition proceeded in two stages: the bulk of the brush collapsed over a broad temperature range and the end of the process was signaled by a sharp first-order transition of the surface of the brush. However, we believe the experiments described here differ from the above-mentioned study in that solvation responsiveness, instead of thermoresponsiveness, was used to trigger the transition. As is well known, in pure water the basis of solubility of PNIPAM is related to the formation of H bonds between H_2O and the amide groups in the polymer. For the occurrence of the LCST, hydrophobic effects are also important.[26] In a water/methanol (50% v/v) PNIPAM ternary system at room temperature, the solvent–solvent interaction due to the formation of water–methanol complexes is stronger than the solvent–polymer interactions, thus leading to the desolvation of PNIPAM.[31,62,63] The timescales of the brush response to solvent change, as described here, provide important information for the application of these materials in the fields of, for example, microfluidics and drug release where responsive systems have potential use.

3. Conclusion

brushes with different grafting densities were synthesized by back-filling defects of inert silane monolayers with SI-ATRP initiators. The effects of co-nonsolvency as well as grafting density on the mechanical properties, more specifically the apparent Young's moduli, of these PNIPAM brushes were studied using an AFM-based colloidal probe nanoindentation method. A fourfold increase in apparent Young's modulus values was observed when PNIPAM brushes were switched from the swollen to the collapsed state. The collapse dynamics of the PNIPAM brushes was investigated by monitoring the change of adherence between the grafts surface and the colloidal probe. A direct correlation was observed between the timescale of the collapse and the thickness of the PNIPAM brush, thus indicating that the factor limiting the response time is the diffusion of solvent in and out of the polymer brushes.

4. Experimental Section

Materials: *N*-Isopropylacrylamide (NIPAM, Aldrich, 97%) was recrystallized twice from a toluene/hexane solution (50% v/v) and dried under vacuum prior to use. Copper(I) bromide (CuBr, Aldrich, 98%) was purified by stirring in glacial acetic acid, filtering, and washing with ethanol three times, followed by drying in vacuum at room temperature overnight. Copper(II) bromide (Sigma–Aldrich, ≥99%), methanol (Biosolve, absolute), *N*,*N*,*N*′,*N*″,*N*″-pentamethyldiethylenetriamine (PMDETA; 98%, Acros Organics), 2-bromo-2-methylpropionic acid (98%, Aldrich), and chlorotrimethylsilane (CTS, Aldrich, ≥97%) were used as received. The ATRP initiator, 3-(chlorodimethylsilyl)propyl 2-bromo-2-methylpropionate (CDB), was synthesized according to a literature procedure.[64] All water used in the experiments was Millipore Milli-Q grade.

Formation of CTS Self-Assembled Monolayers (SAMs): Silicon substrates were first cleaned with piranha solution, then rinsed extensively with water, ethanol, and dichloromethane. *Caution: Piranha solution reacts violently with many organic materials and should be handled with great care!* Dried substrates were immersed in anhydrous toluene solutions (25 mL) containing Et_3N (17.5 μL, 5 mM) and chlorotrimethylsilane (16 μL, 5 mM) was added. Reaction was carried out at room temperature for predetermined times. After rinsing with toluene and ethanol, samples were dried in a nitrogen stream and immediately used for the next step.

ATRP Initiator Vapor-Phase Deposition: ATRP initiator (30 μL) was placed in a glass vial at the bottom of a desiccator, and the substrates with CTS SAMs and cleaned silicon substrates were placed around the vial. The desiccator was then evacuated by a rotary vane pump for 10 min and subsequently closed. Vapor deposition was allowed to proceed for 10 h. Afterwards the substrates were washed with anhydrous toluene, sonicated in ethanol for 1 min, and dried in a nitrogen stream. The substrates were directly used for SI-ATRP experiments.

ATRP of PNIPAM Brushes: NIPAM (5.73 g, 50 mmol) monomer and PMDETA (314 μL, 1 mmol) were added to a mixture of water (18 mL) and methanol (2 mL). The solution was purged with argon for 30 min. CuBr (71.7 mg, 0.5 mmol) and $CuBr_2$ (11.2 mg, 0.05 mmol) were added to another reaction flask and also flushed with argon. Monomer, ligand, and catalyst were then combined and stirred for another 0.5 h to facilitate the formation of the organometallic complex. This solution was then transferred into the flasks containing the substrates covered with SAMs. The flasks were sealed with rubber septa and kept at room temperature under argon. After reaching the desired reaction time, the substrates were removed from the polymerization solution, exhaustively rinsed with water to remove any unreacted and not surface tethered substances, and subsequently dried in a stream of nitrogen. The free polymer formed in a separate vial was collected for gel permeation chromatography (GPC) characterization.

GPC Measurements: GPC was carried out in DMF/LiCl (flow rate 1.0 mL min^{-1}) at 25 °C, using microstyragel columns (bead size 10 μm) with pore sizes of 10^5, 10^4, 10^3, and 10^6 Å (Waters) and a differential refractometer (Waters model 2414). Poly(methyl methacrylate) was used as a standard.

SCA Measurements on PNIPAM Brushes: SCA measurements were performed by the sessile drop technique using an optical contact angle device equipped with an electronic syringe unit (OCA15, Dataphysics, Germany). The sessile drop was deposited onto the surface of the materials with the syringe, and the drop contour was fitted by the Young–Laplace method. At least three different measurements of each sample were performed.

Ellipsometry Measurements on PNIPAM Brushes: The thickness of the brushes in the dry state was measured using a Woollam VASE ellipsometer between 380 and 800 nm at an angle of incidence of 70°. The measurements were performed at 22 °C at 30% relative humidity. The data were averaged over five points at the surface of each sample. The film thickness was determined by assuming a Cauchy layer with a refractive index of 1.47 for the PNIPAM. In situ ellipsometric measurements were conducted using the same instrument with a custom-made liquid cell. The samples were immersed in water or a water/methanol mixture (50% v/v) for at least 15 min to ensure full swelling. The measured values of amplitude ratio upon reflection and phase shift were used to obtain the optical constants of the samples with the standard WVASE 32 software package (J. A. Woollam Co.).

AFM Imaging of PNIPAM Brushes: A Dimension D3100 (Digital Instruments, Veeco–Bruker, Santa Barbara, CA) microscope was operated in tapping mode to obtain the thickness and surface morphology of PNIPAM brushes. The PNIPAM brushes were scratched by tweezers and the height differences between the unscratched and the scratched regions were measured to determine the layer thickness.

AFM Force Measurements: Force measurements were performed in a liquid environment using a NanoScope IIIa multimode atomic force microscope (Digital Instruments/Veeco–Bruker, Santa Barbara, CA, USA) equipped with a standard liquid cell. A silica colloidal probe (Novascan Technologies, Inc., Ames, IA, USA) with a spring constant of 0.050 ± 0.003 N m^{-1} (determined using the thermal tune method) and a diameter of 1.00 ± 0.06 μm (determined by scanning a tip array) was used in the experiments. A typical force measurement was carried out in the so-called force volume imaging mode with a *z*-ramp size of 1 μm, a scan rate of 1 Hz, a deflection trigger of 200 nm, and an image area of 10 μm × 10 μm. To change the solvent environment, Milli-Q water or a water/methanol mixture (50% v/v) was gently injected into the AFM liquid cell from the outlet within 5 s by using a syringe.

Supporting Information

Supporting Information is available from the Wiley Online Library or from the author.

Acknowledgements

This work was financially supported by the MESA+ Institute for Nanotechnology of the University of Twente and the Netherlands Organization for Scientific Research (NWO, TOP Grant 700.56.322, Macromolecular Nanotechnology with Stimulus Responsive Polymers).

This Full Paper is part of the Special Issue on Nanotechnology with Soft Matter.

[1] X. F. Sui, J. Y. Yuan, W. Z. Yuan, M. Zhou, *Prog. Chem.* **2008**, *20*, 1122–1127.
[2] R. Barbey, L. Lavanant, D. Paripovic, N. Schüwer, C. Sugnaux, S. Tugulu, H. A. Klok, *Chem. Rev.* **2009**, *109*, 5437–5527.
[3] P. M. Mendes, *Chem. Soc. Rev.* **2008**, *37*, 2512–2529.
[4] S. Edmondson, V. L. Osborne, W. T. S. Huck, *Chem. Soc. Rev.* **2004**, *33*, 14–22.
[5] K. Matyjaszewski, N. V. Tsarevsky, *Nat. Chem.* **2009**, *1*, 276–288.
[6] S. Minko, *Polym. Rev.* **2006**, *46*, 397–420.
[7] M. A. C. Stuart, W. T. S. Huck, J. Genzer, M. Müller, C. Ober, M. Stamm, G. B. Sukhorukov, I. Szleifer, V. V. Tsukruk, M. Urban, F. Winnik, S. Zauscher, I. Luzinov, S. Minko, *Nat. Mater.* **2010**, *9*, 101–113.
[8] Y. Tsujii, K. Ohno, S. Yamamoto, A. Goto, T. Fukuda, *Adv. Polym. Sci.* **2006**, *197*, 1–45.
[9] O. Smidsrød, J. E. Guillet, *Macromolecules* **1969**, *2*, 272–277.
[10] H. G. Schild, *Prog. Polym. Sci.* **1992**, *17*, 163–249.

[11] I. Luzinov, S. Minko, V. V. Tsukruk, *Soft Matter* **2008**, *4*, 714–725.
[12] A. Synytska, E. Svetushkina, N. Puretskiy, G. Stoychev, S. Berger, L. Ionov, C. Bellmann, K.-J. Eichhorn, M. Stamm, *Soft Matter* **2010**, *6*, 5907–5914.
[13] N. Ishida, S. Biggs, *Macromolecules* **2010**, *43*, 7269–7276.
[14] E. M. Benetti, S. Zapotoczny, J. Vancso, *Adv. Mater.* **2007**, *19*, 268–271.
[15] E. C. Cho, Y. D. Kim, K. Cho, *J. Colloid Interface Sci.* **2005**, *286*, 479–486.
[16] M. A. Cole, N. H. Voelcker, H. Thissen, R. G. Horn, H. J. Griesser, *Soft Matter* **2010**, *6*, 2657–2667.
[17] N. Ishida, S. Biggs, *Langmuir* **2007**, *23*, 11083–11088.
[18] D. M. Jones, J. R. Smith, W. T. S. Huck, C. Alexander, *Adv. Mater.* **2002**, *14*, 1130–1134.
[19] S. Kidoaki, S. Ohya, Y. Nakayama, T. Matsuda, *Langmuir* **2001**, *17*, 2402–2407.
[20] G. Liu, G. Z. Zhang, *J. Phys. Chem. B* **2005**, *109*, 743–747.
[21] I. B. Malham, L. Bureau, *Langmuir* **2010**, *26*, 4762–4768.
[22] S. Mendez, B. P. Andrzejewski, H. E. Canavan, D. J. Keller, J. D. McCoy, G. P. Lopez, J. G. Curro, *Langmuir* **2009**, *25*, 10624–10632.
[23] K. N. Plunkett, X. Zhu, J. S. Moore, D. E. Leckband, *Langmuir* **2006**, *22*, 4259–4266.
[24] H. Yim, M. S. Kent, S. Mendez, G. P. Lopez, S. Satija, Y. Seo, *Macromolecules* **2006**, *39*, 3420–3426.
[25] X. Zhu, C. Yan, F. M. Winnik, D. Leckband, *Langmuir* **2007**, *23*, 162–169.
[26] F. M. Winnik, H. Ringsdorf, J. Venzmer, *Macromolecules* **1990**, *23*, 2415–2416.
[27] H. M. Crowther, B. Vincent, *Colloid Polym. Sci.* **1998**, *276*, 46–51.
[28] H. G. Schild, M. Muthukumar, D. A. Tirrell, *Macromolecules* **1991**, *24*, 948–952.
[29] I. Anac, A. Aulasevich, M. J. N. Junk, P. Jakubowicz, R. F. Roskamp, B. Menges, U. Jonas, W. Knoll, *Macromol. Chem. Phys.* **2010**, *211*, 1018–1025.
[30] M. Kaholek, W. K. Lee, S. J. Ahn, H. W. Ma, K. C. Caster, B. LaMattina, S. Zauscher, *Chem. Mater.* **2004**, *16*, 3688–3696.
[31] G. M. Liu, G. Z. Zhang, *Langmuir* **2005**, *21*, 2086–2090.
[32] E. Meyer, *Prog. Surf. Sci.* **1992**, *41*, 3–49.
[33] X. F. Sui, S. Zapotoczny, E. M. Benetti, P. Schön, G. J. Vancso, *J. Mater. Chem.* **2010**, *20*, 4981–4993.
[34] Y. H. Lin, J. Teng, E. R. Zubarev, H. Shulha, V. V. Tsukruk, *Nano Lett.* **2005**, *5*, 491–495.
[35] M. C. LeMieux, Y. H. Lin, P. D. Cuong, H. S. Ahn, E. R. Zubarev, V. V. Tsukruk, *Adv. Funct. Mater.* **2005**, *15*, 1529–1540.
[36] A. J. Parnell, S. J. Martin, R. A. L. Jones, C. Vasilev, C. J. Crook, A. J. Ryan, *Soft Matter* **2009**, *5*, 296–299.
[37] H. J. Butt, B. Cappella, M. Kappl, *Surf. Sci. Rep.* **2005**, *59*, 1–152.
[38] S. Onclin, B. J. Ravoo, D. N. Reinhoudt, *Angew. Chem. Int. Ed.* **2005**, *44*, 6282–6304.
[39] A. Ulman, *Chem. Rev.* **1996**, *96*, 1533–1554.
[40] I. Choi, Y. Kim, S. K. Kang, J. Lee, J. Yi, *Langmuir* **2006**, *22*, 4885–4889.
[41] L. H. Li, Y. Zhu, B. Li, C. Y. Gao, *Langmuir* **2008**, *24*, 13632–13639.
[42] B. Zdyrko, K. S. Iyer, I. Luzinov, *Polymer* **2006**, *47*, 272–279.
[43] A direct measurement of grafting density and the polymer chain length is rather difficult due to the very small number of polymer chains at surfaces.
[44] S. Edmondson, N. T. Nguyen, A. L. Lewis, S. P. Armes, *Langmuir* **2010**, *26*, 7216–7226.
[45] H. Tu, C. E. Heitzman, P. V. Braun, *Langmuir* **2004**, *20*, 8313–8320.
[46] A. Halperin, *Langmuir* **2010**, *26*, 8933–8940.
[47] S. Kessel, S. Schmidt, R. Müller, E. Wischerhoff, A. Laschewsky, J. F. Lutz, K. Uhlig, A. Lankenau, C. Duschl, A. Fery, *Langmuir* **2010**, *26*, 3462–3467.
[48] E. C. Cho, Y. D. Kim, K. Cho, *Polymer* **2004**, *45*, 3195–3204.
[49] We note that for deformable materials the "zero distance" becomes a matter of definition.[35] There is an error of a few nanometers due to the determination of the point of contact, which is shown in Figure 3a–c.
[50] It should be noted that the obtained Young's modulus value here is the apparent Young's modulus, as the effect of the solid support cannot be neglected, even though only a small amount of deformation was probed.
[51] M. E. McConney, S. Singamaneni, V.V. Tsukruk, *Polym. Rev.* **2010**, *50*, 235–286.
[52] S. Schmidt, M. Zeiser, T. Hellweg, C. Duschl, A. Fery, H. Möhwald, *Adv. Funct. Mater.* **2010**, *20*, 3235–3243.
[53] M. E. Harmon, D. Kucking, C. W. Frank, *Langmuir* **2003**, *19*, 10660–10665.
[54] O. Tagit, N. Tomczak, G. J. Vancso, *Small* **2008**, *4*, 119–126.
[55] E. K. Dimitriadis, F. Horkay, J. Maresca, B. Kachar, R. S. Chadwick, *Biophys. J.* **2002**, *82*, 2798–2810.
[56] H. Shulha, A. Kovalev, N. Myshkin, V. V. Tsukruk, *Eur. Polym. J.* **2004**, *40*, 949–956.
[57] D. Filip, V. I. Uricanu, M. H. G. Duits, W. G. M. Agterof, J. Mellema, *Langmuir* **2005**, *21*, 115–126.
[58] For this film, the stress field does not decay within the brush; thus there is a finite force acting on the substrate which will influence the modulus measured.
[59] Here we use "adherence" to describe the practical work of adhesion to emphasize differences between its value and the magnitude of thermodynamic adhesion. The latter, if expressed in work of adhesion, corresponds to the reversible free energy change per unit surface area when two contacting surfaces are moved apart from contact to infinite distance of separation. Thus, adherence also includes the energy dissipated during separation of the contacting surfaces from each other.
[60] S. Yamamoto, M. Ejaz, Y. Tsujii, T. Fukuda, *Macromolecules* **2000**, *33*, 5608–5612.
[61] X. Laloyaux, B. Mathy, B. Nysten, A. M. Jonas, *Langmuir* **2010**, *26*, 838–847.
[62] G. Z. Zhang, C. Wu, *J. Am. Chem. Soc.* **2001**, *123*, 1376–1380.
[63] J. K. Hao, H. Cheng, P. Butler, L. Zhang, C. C. Han, *J. Chem. Phys.* **2010**, *132*, 154902.
[64] B. Lego, W. G. Skene, S. Giasson, *Langmuir* **2008**, *24*, 379–382.

Received: December 10, 2010
Revised: January 17, 2011
Published online: April 20, 2011

